

Bureau International des Poids et Mesures

**Comparison of the standards for air kerma
of the ENEA-INMRI and the BIPM for ^{60}Co gamma rays**

P J Allisy-Roberts, D T Burns, C Kessler
BIPM

R F Laitano, M Bovi, M Pimpinella and M P Toni,
ENEA-INMRI



September 2005

Pavillon de Breteuil, F-92312 SEVRES cedex

**Comparison of the standards for air kerma
of the ENEA-INMRI and the BIPM for ^{60}Co γ -rays**

P.J. Allisy-Roberts, D.T. Burns and C. Kessler
Bureau International des Poids et Mesures, F-92312 Sèvres Cedex,
France

R.F. Laitano, M. Bovi, M. Pimpinella and M.P. Toni,
Istituto Nazionale di Metrologia delle Radiazioni Ionizzanti,
ENEA CR Casaccia, cp 2400 – 00100 Rome, Italy

Abstract

A new comparison of the standards for air kerma of the Istituto Nazionale di Metrologia delle Radiazioni Ionizzanti of the Ente per le Nuove Tecnologie, l'Energia e l'Ambiente, Italy (ENEA-INMRI) and of the Bureau International des Poids et Mesures (BIPM) has been carried out in ^{60}Co radiation. The comparison result, expressed as a ratio of the ENEA and BIPM standards, is 1.0051 (0.0026).

1. Introduction

A new comparison of the standards for air kerma of the Istituto Nazionale di Metrologia delle Radiazioni Ionizzanti of the Ente per le Nuove Tecnologie, l'Energia e l'Ambiente, Italy, and of the Bureau International des Poids et Mesures, was carried out at the BIPM in ^{60}Co radiation in December 2004. In this comparison, the ENEA-INMRI used a series of four graphite cavity ionization chambers constructed at the ENEA-INMRI and described in section 2 of this report. The BIPM air kerma standard is described in [1].

Previous comparisons between the ENEA-INMRI and the BIPM were made in 1983 [2] and 1998 (revised in 2003) [3, 4] and a bilateral comparison between the National Institute of Standards and Technology (NIST), USA, and the ENEA-INMRI was conducted in 1994 [5]. The results of these earlier comparisons are consistent when the various changes related to chamber volumes and wall correction factors are taken into account, as discussed later in this report.

2. Determination of the air kerma

The air kerma rate is determined by

$$\dot{K} = \frac{I}{m} \frac{W}{e} \frac{1}{1-\bar{g}} \left(\frac{\mu_{\text{en}}}{\rho} \right)_{\text{a,c}} \bar{s}_{\text{c,a}} \prod k_i \quad , \quad (1)$$

where

- I/m is the ionization current per unit mass of air measured by the standard,
- W is the average energy spent by an electron of charge e to produce an ion pair in dry air,
- \bar{g} is the fraction of electron energy lost in bremsstrahlung production in air,
- $(\mu_{\text{en}}/\rho)_{\text{a,c}}$ is the ratio of the mean mass energy-absorption coefficients of air and graphite,
- $\bar{s}_{\text{c,a}}$ is the ratio of the mean stopping powers of graphite and air,
- $\prod k_i$ is the product of the correction factors to be applied to the standard.

Figure 1 illustrates the series of six chambers made at the ENEA-INMRI to determine air kerma and verify the various correction factors. The main characteristics of the ENEA-INMRI standards are given in Table 1. The standard chamber code F is used as the primary standard. The other standards, which differ in dimensions, are used to verify the calculated correction factors. However, chambers D and E – being very similar to chamber F – were not taken to the BIPM for the present comparison.

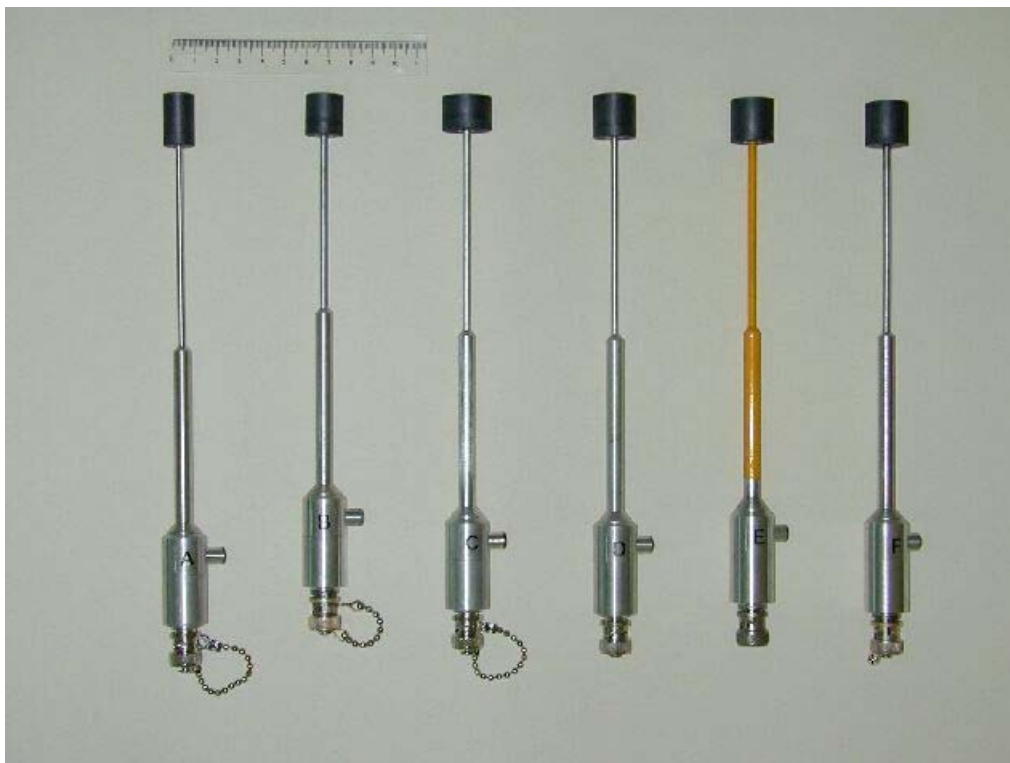


Figure 1. Photograph of the six cavity chambers made at the ENEA-INMRI. From the left the chambers are coded A, B, C, D, E and F, respectively. The chambers used in the present comparison are A, B, C and F.

Table 1. Dimensions and relevant parameters of the ENEA-INMRI standard chambers (reference date 06.01.2004)

| ENEA-INMRI Standard Chambers ⁽¹⁾ | | | | | | | |
|---|---|-------------|-------------|-------------|-------------|--------------------|--------------------|
| | A | B | C | D | E | F | |
| Chamber dimensions | | | | | | | |
| Inner diameter (mm) | 7.98 | 10.87 | 16.01 | 11.00 | 11.00 | 11.00 | |
| Inner length (mm) | 15.98 | 10.86 | 7.97 | 11.02 | 10.97 | 11.03 | |
| Lateral wall thickness (mm) | 3.0 | 3.0 | 3.0 | 4.0 | 4.0 | 4.0 | |
| Upper base thickness (mm) | 2.97 | 2.99 | 3.00 | 3.88 | 3.99 | 3.97 | |
| Lower base thickness (mm) | 4.00 | 4.00 | 3.99 | 4.0 | 4.0 | 4.00 | |
| Central electrode diameter (mm) | 1.96 | 1.99 | 1.99 | 1.98 | 2.00 | 2.00 | |
| Central electrode length (mm) | 14.98 | 10.07 | 7.01 | 10.00 | 10.12 | 10.13 | |
| Air cavity volume (cm ³) | 0.77206 (93) | 0.9881 (12) | 1.5983 (19) | 1.0324 (12) | 1.0223 (12) | 1.0287 (12) | |
| Correction factors and physical parameters | | | | | | | |
| Polarizing tension (V) (both polarities) | 300 | | | | | | |
| Chamber material (wall and central electrode) | graphite (1.75 g cm ⁻³) | | | | | | |
| $I+/I-$ | 1.0025 (7) | 1.0027 (7) | 1.0010 (7) | 1.0026 (7) | 1.0022 (7) | 1.0014 (7) | |
| $\bar{S}_{c,a}$ | 1.0008 | 1.0007 | 1.0006 | 1.0007 | 1.0007 | 1.0007 | |
| $k_{pn} \cdot k_{nppn}$ ⁽²⁾ | 1.0005 (14) | 1.0001 (14) | 0.9996 (14) | 1.0001 (14) | 1.0001 (14) | 1.0001 (14) | |
| k_{wall} ⁽³⁾ | 1.0116 (10) | 1.0161 (10) | 1.0271 (10) | 1.0212 (10) | 1.0212 (10) | 1.0212 (10) | |
| ENEA 36 TBq beam (reference date 06.01.2004) | k_{sat} ⁽²⁾ | 1.0011 (5) | 1.0017 (5) | 1.0047 (5) | 1.0019 (5) | 1.0019 (5) | 1.0019 (5) |
| | \dot{K}_a (mGy s ⁻¹) ⁽⁴⁾ | 2.0500 (61) | 2.0440 (61) | 2.0459 (61) | 2.0445 (61) | 2.0441 (61) | 2.0454 (61) |
| ENEA 208 TBq beam (reference date 04.01.2005) | k_{sat} ⁽²⁾ | 1.0013 (5) | 1.0020 (5) | 1.0092 (5) | 1.0021 (5) | 1.0021 (5) | 1.0021 (5) |
| | \dot{K}_a (mGy s ⁻¹) ⁽⁴⁾ | 12.790 (38) | 12.751 (38) | 12.797 (38) | 12.772 (38) | 12.762 (38) | 12.771 (38) |

⁽¹⁾ The figures in parentheses are the values of the combined standard uncertainty.

⁽²⁾ According to the ENEA air kerma rates.

⁽³⁾ Values obtained by Monte Carlo determination ($s = 10^{-4}$) at a source-chamber distance of 100 cm in the new ENEA 208 TBq beam.

⁽⁴⁾ Values of the air kerma rate obtained as the arithmetic mean of measurements made in the period from March 2003 until June 2004 for the ENEA 36 TBq beam and from March until April 2005 for the ENEA 208 TBq beam. The relative standard deviation associated with each value was up to 10^{-4} (with 580 degrees of freedom), depending on the chamber.

3. Experimental results

The air kerma is determined at the BIPM under the following conditions:

- the distance from source to reference plane is 1 m;
- the field size in air at the reference plane is 10 cm × 10 cm, the photon fluence rate at the centre of each side of the square being 50 % of the photon fluence rate at the centre of the square.

Data concerning the various factors entering in the determination of air kerma in the ^{60}Co beam using the primary standards of the ENEA-INMRI and the BIPM are shown in Table 2. They include the physical constants [6], the correction factors entering in (1), the volume of each chamber cavity and the associated uncertainties.

Table 2. Physical constants and correction factors entering in the determination of air kerma and their estimated relative uncertainties in the BIPM ^{60}Co 23 TBq beam

| | BIPM values | Relative uncertainty ^(a) | | ENEA-INMRI values | Relative uncertainty ^(a) | | R_K relative uncertainty ^(a) | |
|--|-----------------------|-------------------------------------|---------------------|-----------------------|-------------------------------------|---------------------|---|-----------|
| | | 100 s_i | 100 u_i | | 100 s_i | 100 u_i | 100 s_i | 100 u_i |
| Physical constants | | | | | | | | |
| dry air density / $\text{kg}\cdot\text{m}^{-3}$ ^(b) | 1.2930 | – | 0.01 | 1.2930 | – | 0.01 | – | – |
| $(\mu_{\text{en}}/\rho)_{\text{a.c}}$ | 0.9985 | – | 0.05 | 0.9985 | – | 0.05 | – | – |
| $\bar{s}_{\text{c,a}}$ | 1.0010 | – | 0.11 ^(c) | 1.0007 | – | 0.11 ^(c) | – | – |
| W/e | 33.97 | – | – | 33.97 | – | – | – | – |
| \bar{g} | 0.0032 | – | 0.02 | 0.0032 | – | 0.02 | – | – |
| Correction factors | | | | | | | | |
| k_{s} recombination loss | 1.0015 ^(d) | 0.01 | 0.01 | 1.0017 ^(d) | – | 0.02 | 0.01 | 0.02 |
| k_{h} humidity | 0.9970 | – | 0.03 | 0.9970 | – | 0.03 | – | – |
| k_{st} stem scattering | 1.0000 | 0.01 | – | 1.0000 | – | 0.03 | 0.01 | 0.03 |
| k_{att} wall attenuation | 1.0398 | 0.01 | 0.04 | – | – | – | – | – |
| k_{sc} wall scattering | 0.9720 | 0.01 | 0.07 | 1.0212 | – | 0.10 | 0.01 | 0.13 |
| k_{CEP} mean origin of electrons | 0.9922 | – | 0.01 | – | – | – | – | – |
| k_{an} axial non-uniformity | 0.9964 | – | 0.07 | 1.0001 | – | 0.14 | – | 0.16 |
| k_{rn} radial non-uniformity | 1.0016 ^(e) | 0.01 | 0.04 | 1.0003 ^(e) | – | 0.01 | 0.01 | 0.04 |
| Measurement of $I/V\rho$ | | | | | | | | |
| V volume / cm^3 | 6.8028 | 0.01 | 0.03 | 1.0287 | – | 0.12 | 0.01 | 0.12 |
| I ionization current / pA ^(b) | – | 0.01 | 0.02 | 70.795 | 0.01 | 0.03 | 0.01 | 0.04 |
| Uncertainty | | | | | | | | |
| quadratic summation | – | 0.03 | 0.17 | – | 0.01 | 0.25 | 0.03 | 0.25 |
| combined uncertainty | – | 0.17 | | – | 0.25 | | 0.26 | |

^(a) Expressed as one standard deviation.

s_i represents the relative uncertainty estimated by statistical methods, type A,

u_i represents the relative uncertainty estimated by other means, type B.

^(b) At 101.325 kPa and 273.15 K.

^(c) Combined uncertainty for the product of stopping power ratio and W/e

^(d) This correction is 1.0019 (1) for the BIPM standard and 1.0019 (2) for the ENEA-INMRI standard in the 175 TBq beam

^(e) The radial non-uniformity correction is 1.0015 (2) for the BIPM standard and 1.0002 (1) for the ENEA-INMRI standard in the 175 TBq beam.

For the BIPM standard, these data are taken from [7]. Also shown in Table 2 are the relative uncertainties in the ratio

$$R_K = \dot{K}_{\text{ENEA-INMRI}} / \dot{K}_{\text{BIPM}}. \quad (2)$$

Two different ^{60}Co beams were used at the BIPM (the 23 TBq old source and the 175 TBq new source). Similarly at the ENEA-INMRI, two different ^{60}Co beams were used (the 36 TBq old source and the 208 TBq new source). Table 3 gives the differences between the characteristics of the ENEA-INMRI ^{60}Co beams and those at the BIPM.

Table 3. Parameters of the ^{60}Co beams at the ENEA-INMRI and the BIPM

| ^{60}Co beam | Nominal source activity at 01/01/04 | Source diameter | Scatter contribution/energy fluence | Field size at 1 m |
|-----------------------|-------------------------------------|-----------------|-------------------------------------|-------------------|
| ENEA old source | 36 TBq | 15 mm | 18 % | 10 cm × 10 cm |
| ENEA new source | 208 TBq | 20 mm | 14 % | 10 cm × 10 cm |
| BIPM old source | 23 TBq | 20 mm | 14 % | 10 cm × 10 cm |
| BIPM new source | 175 TBq | 20 mm | 21 % | 10 cm × 10 cm |

The correction factors for the ENEA-INMRI primary standard-F were determined at the ENEA-INMRI. The accuracy of the volume determination and of the calculated correction factors was verified by the ratio of air kerma measurements made by all six chambers at the ENEA-INMRI.

The polarity effect determined at the ENEA-INMRI for the primary standard-F was 1.0014 (7). A similar value was determined at the BIPM for this chamber and of the same order for the other chambers, being smaller than that at the ENEA-INMRI. However, as all measurements were made with both polarities no corrections for this were applied.

The correction k_s for ion recombination was first determined in the ENEA 36 TBq old beam by the method [8]. This correction was then re-determined by the same method but using also the new 208 TBq beam and hence a wider range of air kerma rates. The ratios of ionization currents, for the determination of k_s , were obtained at chamber potentials of 300 V and 75 V (both polarities). The results of ion recombination measurements made at the ENEA-INMRI are reported in Table 4. The values of k_s for the different ENEA chambers in the two ENEA beams are given in Table 1. These values differ by up to 3×10^{-4} from those previously determined at a lower range of air kerma rates, by using just the ENEA 36 TBq beam.

Measurements concerning the effect of ion recombination were repeated in the BIPM beams. The ratio of the ionization currents obtained with applied voltages of 300 V and 100 V (both polarities) $I_V / I_{V/3}$ [8] in the BIPM beams was measured for a series of different air kerma rates to determine the value of k_s . The results are illustrated in Figure 2 and given in Table 4. Some differences of up to 7×10^{-4} in relative terms were identified between the ENEA and BIPM determinations of k_s for some of the chambers. Consequently, the values used for this comparison in the BIPM beams and given in Table 2 are those measured at the BIPM.

The correction $k_s = 1.0017$ (0.0001) as measured at the BIPM was applied to the ENEA-INMRI standard-F in the BIPM 23 TBq beam and $k_s = 1.0019$ (0.0001) in the 175 TBq beam. The values calculated from the ENEA-INMRI measurements gave 1.0020 (5) and 1.0022 (5) respectively.

Figure 2 Graphs of recombination measurements made at the BIPM

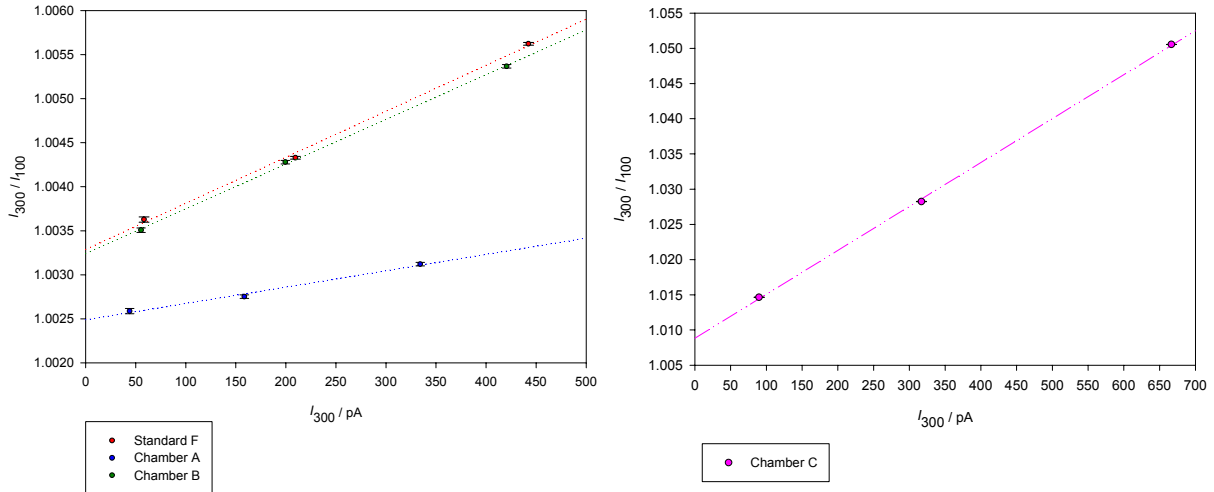


Table 4 Results of ion recombination measurements made at the BIPM and at the ENEA-INMRI for the ENEA-INMRI standards

| ENEA-INMRI Standard | A | B | C | F |
|---|----------------------|----------------------|----------------------|----------------------|
| Initial recombination and diffusion, BIPM values | 12×10^{-4} | 16×10^{-4} | 44×10^{-4} | 16×10^{-4} |
| Initial recombination and diffusion, ENEA-INMRI values | 12×10^{-4} | 17×10^{-4} | 39×10^{-4} | 19×10^{-4} |
| Volume recombination factor, BIPM values / pA^{-1} | 2.3×10^{-7} | 6.4×10^{-7} | 7.8×10^{-6} | 6.5×10^{-7} |
| Volume recombination factor, ENEA-INMRI values / pA^{-1} | 1.6×10^{-7} | 6.3×10^{-7} | 7.5×10^{-6} | 5.1×10^{-7} |
| k_s in the BIPM 23 TBq beam, BIPM values | 1.0013 (1) | 1.0017 (1) | 1.0051 (5) | 1.0017 (1) |
| k_s in the BIPM 175 TBq beam, BIPM values | 1.0013 (1) | 1.0019 (1) | 1.0096 (8) | 1.0019 (1) |

The effect of attenuation and scatter in the graphite walls of the ENEA-INMRI chambers was formerly determined by Monte Carlo calculation [9, 10] in the old ENEA beam. A new k_{wall} determination was made using the ^{60}Co photon spectrum obtained by a Monte Carlo simulation of the new ENEA 208 TBq beam. The results are reported in Table 1. On this occasion a study on the dependence of k_{wall} on the spectrum shape was also made [11]. To this end a number of spectra were considered, with a scatter component ranging from 14 % to 21 % (the same range as that referred to in Table 3). In this range the value for k_{wall} varied by not more than 8×10^{-4} , depending on the chamber.

The new k_{wall} value of 1.0212 ($s = 1 \times 10^{-4}$), adopted for the ENEA-INMRI primary standard-F, differs by 7×10^{-4} from the value of 1.0219 ($s = 1 \times 10^{-4}$) calculated for a similar (but not identical) chamber at the National Research Council (NRC), Canada [12] using the same Monte Carlo code EGSnrc. The two determinations are slightly different because of some differences in the ^{60}Co photon spectra and chamber dimensions used in the two calculations.

An additional correction factor k_m for the radial non-uniformity of the BIPM beam over the cross-section of the ENEA-INMRI standard-F has been estimated from [13]; its numerical value is 1.0003 (1) in the 23 TBq beam and 1.0002 in the 175 TBq beam, as given in Table 5.

Table 5. Results of radial non-uniformity calculations made at the BIPM for the ENEA-INMRI standards

| ENEA-INMRI Standard | A | B | C | F |
|---------------------------|------------|------------|------------|------------|
| k_m in the 23 TBq beam | 1.0006 (1) | 1.0003 (1) | 1.0002 (1) | 1.0003 (1) |
| k_m in the 175 TBq beam | 1.0004 (1) | 1.0002 (1) | 1.0002 (1) | 1.0002 (1) |

Before the comparison each ENEA chamber was measured at the ENEA in the 36 TBq beam in the period from March 2003 until June 2004. The maximum deviation obtained among the mean values of 20 series (30 measurements each) was within 4×10^{-4} depending on the chamber. No particular trends were observed for the various chambers. Each chamber was set up and measured in each of the BIPM beams on at least two separate occasions. The results were reproducible to within 10^{-4} . All the chambers were re-measured 10 weeks later at the BIPM. Chambers A and F were consistent to within 10^{-4} whereas chambers B and C appeared to have drifted by 3×10^{-4} . After measurements at the BIPM, the chambers were measured at the ENEA in the 208 TBq beam and also re-measured after a period of 5 weeks. The reproducibility of these two series of measurements was within 2×10^{-4} and thus consistent with previous measurements.

The evaluation of the air kerma rate at the BIPM measured with the ENEA-INMRI primary standard-F is obtained from (1) in section 2 using the data in Table 2 and the mean measured ionization current in each of the BIPM beams. A similar comparison has been made for each of the other three chambers to verify the correction factors used. The corrections that have been applied for each chamber in the two beams are given in Table 4 for recombination and Table 5 for radial non-uniformity. The comparison results are given in Table 6.

For consistency with all previous comparisons, the \dot{K}_{BIPM} value is taken as the mean of four measurements made before and after the comparison for the 23 TBq beam, and over the last two years, since its installation, for the 175 TBq beam. Both air kerma rates were verified during the comparison. The \dot{K} values refer to an evacuated path length between source and standard and are given at the reference date of 2004-01-01, 0 h UTC where the half-life of ^{60}Co is taken as 1925.5 days ($u = 0.5$ days) [14].

Table 6. The experimental results from the four ENEA-INMRI chambers in the two BIPM beams

| ENEA-INMRI Chamber | 23 TBq beam result | 175 TBq beam result | Ratio of the 23 TBq to the 175 TBq result |
|--------------------------------|---|---|---|
| | $\dot{K}_{\text{ENEA-INMRI}} / \text{mGy s}^{-1}$ | $\dot{K}_{\text{ENEA-INMRI}} / \text{mGy s}^{-1}$ | |
| A | 1.8521 | 14.1474 | 13.091×10^{-2} |
| B | 1.8459 | 14.0940 | 13.097×10^{-2} |
| C | 1.8518 | 14.1393 | 13.097×10^{-2} |
| F | 1.8491 | 14.1216 | 13.094×10^{-2} |
| Mean values | 1.8497 (23) | 14.126 (19) | 13.095×10^{-2} (3) |
| \dot{K}_{BIPM} values | 1.8396 ₅ | 14.057 ₉ | $13.086_2 \times 10^{-2}$ |

The results of the measurements with the four ENEA-INMRI standard chambers in the two BIPM beams indicate relative differences of up to 3.8×10^{-3} between the four ENEA-INMRI standards' responses in terms of air kerma. The chambers were consistent in their individual measurements during the comparison at the BIPM. The spread of the results is of the same order of the spread of 3.6×10^{-3} determined at the ENEA.

The overall results of the four chambers are given in Table 7 in terms of a comparison result. The results for all four chambers relative to the BIPM are systematically lower in the 175 TBq BIPM beam than in the 23 TBq beam, from about 3×10^{-4} to 8×10^{-4} . This is within the uncertainties of the differences in the correction factors.

Table 7. Results of the ENEA-INMRI/BIPM comparison for standards of air kerma

| ENEA-INMRI chamber | $\dot{K}_{\text{ENEA-INMRI}} / \dot{K}_{\text{BIPM}}$ | |
|--------------------|---|-------------------|
| | BIPM 23 TBq beam | BIPM 175 TBq beam |
| A | 1.0067 | 1.0064 |
| B | 1.0034 | 1.0026 |
| C | 1.0066 | 1.0058 |
| F | 1.0051 | 1.0045 |

The air kerma results of the A, B and C ENEA-INMRI chambers relative to the primary standard-F are shown in Table 8. These ratios make it possible to check the consistency of the ENEA-INMRI chamber results in each of the four gamma beams used at ENEA and BIPM. For the present purpose the ratios to be compared with each other are those referring to a given chamber in the different beams (each row in Table 8). Ideally these ratios should be constant irrespective of the beams. The differences obtained are up to 0.7×10^{-3} , 1.4×10^{-3} and 1.8×10^{-3} for chambers A, B and C, respectively. These differences are within the combined standard uncertainty.

Table 8. Results for the ENEA-INMRI chambers A, B and C relative to the primary standard-F in the BIPM and the ENEA beams.

| ENE INMRI Chamber | Ratio of the chamber result to chamber F | | | | Maximum difference |
|-------------------------|--|-------------------------|--|---|-----------------------|
| | BIPM 23 TBq beam | BIPM 175 TBq beam | ENE 36 TBq beam (¹) | ENE 208 TBq beam (¹) | |
| A | 1.0016 (15) | 1.0018 (15) | 1.0022 (17) | 1.0015 (17) | 0.7×10^{-3} |
| B | 0.9983 (5) | 0.9980 (5) | 0.9994 (6) | 0.9985 (6) | 1.4×10^{-3} |
| C | 1.0015 (15) | 1.0013 (15) | 1.0002 (17) | 1.0020 (17) | 1.8×10^{-3} |
| F | 1 | | | | - |

(¹) The combined standard uncertainty (figures in parentheses) on the results for chambers A, B and C relative to the primary standard-F was estimated by combining the uncorrelated components of the uncertainty associated with the factors k_s , k_{wall} (0.03 % spectra, 0.01 % statistical), k_{pn} , k_{npt} and the statistical standard uncertainty on the air density and ionization current measurement. In the case of chamber B some uncertainty components (such as k_s , k_{pn} and k_{npt}) were not considered as this chamber has a very similar geometry to chamber F.

The final result of the comparison using the ENEA-INMRI primary standard-F in the 23 TBq BIPM beam is given in Table 9. The 23 TBq beam has been used for the final result to ensure consistency world-wide as this beam has been used for all the other BIPM.RI(I)-K1 comparison results to date.

Table 9. Final Result of the ENEA-INMRI/BIPM comparison for standards of air kerma

| BIPM beam | $\dot{K}_{ENE-INMRI} / \text{mGy s}^{-1}$ | $\dot{K}_{BIPM} / \text{mGy s}^{-1}$ | R_K | u_c |
|-----------|---|--------------------------------------|--------|--------|
| 23 TBq | 1.8491 | 1.8396 ₅ | 1.0051 | 0.0026 |

The mean ratio of the values of the air kerma rate determined by the ENEA-INMRI and the BIPM standards is 1.0051 with a combined standard uncertainty, u_c , of 0.0026. Some of the uncertainties in \dot{K} that appear in both the BIPM and the ENEA-INMRI determinations (such as air density, W/e , μ_{en}/ρ , \bar{g} , $\bar{s}_{c,a}$ and k_h) cancel when evaluating the uncertainty of R_K as given in Table 2.

The use, at the ENEA, of additional standard chambers providing independent and consistent results increases confidence in the experimental results and the uncertainty analysis.

4. Discussion

4.1 Consistency of comparisons of the ENEA-INMRI standard for air kerma

Previous comparisons between the ENEA-INMRI and the BIPM were made in 1983 [2, 14] (revised in 1985) and 1998 (revised in 2003) [4] and a bilateral comparison between the NIST (USA) and the ENEA-INMRI was conducted in 1994 [5]. The results of these earlier comparisons are consistent with each other within the uncertainties. The present result is consistent with the 2003 revised result and consequently with the earlier results when the various changes related to chamber volume, beam non-uniformity and wall correction factors [16, 17] are taken into account. Table 10 illustrates this evolution.

Table 10. Previous comparison results for the ENEA-INMRI/BIPM

| Year | 1983/85 ⁽¹⁾ | 1994/96 ⁽²⁾ | 1998 result with unrevised parameters ⁽³⁾ | 1998/2003 revision | Present result |
|-------------------|------------------------|------------------------|--|-----------------------|-----------------------|
| ENEA-INMRI/BIPM | 0.9994 ⁽⁴⁾ | 0.9984 ⁽⁴⁾ | 1.0016 ⁽⁴⁾ | 1.0044 ⁽⁴⁾ | 1.0051 ⁽⁵⁾ |
| Uncertainty u_c | 0.0040 | 0.0051 | 0.0026 | 0.0026 | 0.0026 |

(1) The published comparison result of 1983 has been updated to account for the correct value for Δ and then for changes in stopping power ratios in 1985.

(2) The result obtained indirectly through the comparison with the ENEA-INMRI/NIST comparison in 1994 and the NIST/BIPM comparison in 1996 [18].

(3) The variation was in part due to the change in the ^{60}Co source (and source housing) used for air kerma comparisons at the BIPM during the intervening fifteen years

(4) ENEA-INMRI primary standard chamber C1

(5) ENEA-INMRI primary standard chamber F

4.2 Analysis of the BIPM air kerma comparisons

The results of air kerma comparisons in ^{60}Co at the BIPM are currently being re-evaluated, taking into account the effect of changes being made in national standards following the recommendations of the Consultative Committee for Ionizing Radiation (CCRI) [19]. The OMH (Hungary) has already declared a new value for its air kerma standard [20], as have the PTB (Germany) [21] and the BEV (Austria) [22]. The SZMDM (Yugoslavia) and the NCM (Bulgaria), both of which have made comparisons recently with the BIPM [23, 24], have also changed their method of k_{wall} determination, using Monte Carlo calculations. The LNMRI/IRD has recently confirmed their earlier comparison results [25] but is currently in the process of recalculating wall effects for their primary standard which has a similar shape and size to the ENEA-INMRI standard.

The BIPM is also making calculations of the various factors for its standard to verify its determination of air kerma [26]. At present, particularly with a proposed change to the value used for k_{an} , the combined effect would be to increase the BIPM evaluation by 1.0046. The paper in which the calculation methodology and results are given has been submitted for publication [27]. However, any future new result will need to be approved and implemented at a date to be confirmed by the CCRI.

Once all the evaluations have been completed and the results approved by the CCRI, they will be published in the BIPM key comparison database (KCDB) that was set up under the CIPM Mutual Recognition Arrangement [28].

5. Conclusion

The ENEA-INMRI standard for air kerma in ^{60}Co gamma radiation compared with the BIPM air kerma standard gives a comparison result of 1.0051 (0.0026). The differences between this result and those obtained between 1983 and 2003 are consistent with the changes that have been made to the ENEA-INMRI standard.

In principle, all the comparison results of the national metrology institutes and designated laboratories (NMIs) will be used as the basis of the entries in Appendix B of the KCDB set up under the CIPM MRA. The NMIs that have previously used experimental extrapolation methods to determine wall correction factors are currently checking their factors, using various Monte Carlo codes or other methods. It may be some months before all the NMIs will be ready for their results to be entered into the BIPM KCDB. In the meantime, the BIPM is also reviewing its experimental and calculated results for the wall and other corrections of its primary standard.

References

- [1] Boutillon M. and Niatel M.-T., A study of a graphite cavity chamber for absolute measurements of ^{60}Co gamma rays, 1973, [Metrologia](#), **9**, 139-146.
- [2] Allisy A. Comparison of standards of exposure, *Comité Consultatif pour les Étalons de Mesures des Rayonnements Ionisants, Section (I)*, 1983, **7**, p. R(I) 30-31.
- [3] Allisy-Roberts P.J., Toni M., Bovi M., Comparison of the standards for air kerma of the ENEA-INMRI and the BIPM for ^{60}Co γ rays, 2002, [Rapport BIPM-2002/09](#), 10 pp.
- [4] Allisy-Roberts P.J., Burns D.T., Laitano R.F., Toni M., Bovi M., Revised comparison of the standards for air kerma of the ENEA-INMRI and the BIPM for ^{60}Co gamma rays, [Rapport BIPM-2003/10](#), 11 pp.
- [5] Laitano R.F., Lamperti P.J. and Toni M.P. Comparison of the NIST and ENEA air kerma standards, 1994, *ENEA Internal Report*, 33 pp.
- [6] *Comité Consultatif pour les Étalons de Mesures des Rayonnements Ionisants*, Constantes physiques pour les étalons de mesure de rayonnement, 1985, *CCEMRI Section (I)*, **11**, R45.
- [7] Allisy-Roberts P.J., Burns D.T., Kessler C., Measuring conditions used for the calibration of ionization chambers at the BIPM, 2004, [Rapport BIPM-04/17](#), 20 pp.
- [8] Boutillon M. Volume recombination parameter in ionization chambers, 1998, *Phys.Med.Biol.*, **43**, 2061-2072.
- [9] Laitano R.F., Toni M.P., Pimpinella M. and Bovi M. determination of the k_{wall} correction factor for a cylindrical ionization chamber to measure air kerma in a Co-60 gamma beam, 2002, *Phys.Med.Biol.*, **47**, No.14, 2411-2431.
- [10] Laitano R. F., Pimpinella M., Toni M. P. and Tricomi G. Determination of the K_{wall} correction factor for cylindrical ionisation chambers of various dimensions, 2003, *CCRI(I) 16th meeting document* [CCRI\(I\)/03-27](#), 4 pp.
- [11] Pimpinella M., Influence of photon energy spectra on k_{wall} factor and related uncertainty in Co-60 air-kerma measurement by cavity ionization chambers, presented at the CCRI(I) [Workshop on Dosimetry Uncertainties](#), 2005.
- [12] Rogers D.W.O. and Treurniet J. Monte Carlo calculated wall and axial non-uniformity corrections for primary standards of air kerma, 1999, [NRCC Report PIRS-663](#), and *CCRI 14th meeting document* CCRI(I)/99-26, 25 pp.
- [13] Boutillon M. and Perroche A.-M., Radial non-uniformity of the BIPM ^{60}Co beam, 1989, [Rapport BIPM-89/2](#), 9 pp.
- [14] IAEA, X- and gamma-ray standards for detector calibration, 1991, *IAEA TECDOC-619*.
- [15] Laitano R. F. and Toni M. P., The primary exposure standard of ENEA for Co-60 gamma radiation: characteristics and measurement procedures, 1983, *ENEA report*, RT/PROT(83)28.
- [16] Laitano R. F., Physical parameters, correction factors and comparison results for the ENEA air kerma standard for Co-60 gamma rays, 2001, *CCRI(I) 15th meeting document*, [CCRI\(I\)/01-40](#), 1 p.

- [17] Laitano R. F., Pimpinella M., Toni M. P., Quini M., Bovi M., Re-determination of the air-cavity volume for the Co-60 gamma-ray air-kerma standard at the ENEA-INMRI, 2003, *CCRI(I) 16th meeting document* [CCRI\(I\)/03-26](#), 6 pp.
- [18] Allisy-Roberts P.J., Boutillon M., Lamperti P., Comparison of the standards of air kerma of the NIST and the BIPM for ^{60}Co gamma rays, 1996, *Rapport BIPM-1996/09*, 8 pp.
- [19] *Comité Consultatif des Rayonnements Ionisants*, The estimation of k_{att} , k_{sc} k_{CEP} and their uncertainties, 1999, [CCRI, 16, 145-146](#).
- [20] Csete I., New correction factors for the OMH air kerma standard for ^{137}Cs and ^{60}Co radiation, 2001, *CCRI(I) 15th meeting document* [CCRI\(I\)/01-03](#), 2 pp.
- [21] Kramer H.-M., Büermann L. and Ambrosi P. Change in the realization of the gray at the PTB, 2002, *Metrologia*, **39**, 111-112.
- [22] Witzani J., Gabris F., Leitner A., Change of air kerma standards of the BEV for ^{137}Cs and ^{60}Co gamma rays, 2004, *Metrologia*, **41**, L1 –L2.
- [23] Allisy-Roberts P.J., Burns D.T., Kessler C. and Spasić-Jokić V. Comparison of the standards of air kerma of the SZMDM Yugoslavia and the BIPM for ^{60}Co γ rays, 2002, *Rapport BIPM-02/01*, 9 pp.
- [24] Allisy-Roberts P.J., Burns D.T., Kessler C., Ivanov R.N., Comparison of the standards of air kerma of the NCM Bulgaria and the BIPM for ^{60}Co γ rays, 2002, *Rapport BIPM-02/03*, 9 pp.
- [25] Allisy-Roberts P.J., Kessler C., Mello da Silva C.N., Comparison of the standards for air kerma of the LNMRI and the BIPM for ^{60}Co γ rays, *Rapport BIPM-2005/01*, 6 pp.
- [26] Burns D.T., Calculation of k_{wall} for ^{60}Co air-kerma standards using PENELOPE, 2003, *CCRI (I) 16th meeting document*, [CCRI\(I\)/03-40](#), 3 pp.
- [27] Burns D.T., A new approach to the determination of air kerma using primary-standard cavity ionization chambers, submitted to *Physics in Medicine and Biology*, 2005.
- [28] MRA: *Mutual recognition of national measurement standards and of calibration and measurement certificates issued by national metrology institutes*, International Committee for Weights and Measures, 1999, 45 pp. <http://www.bipm.org/pdf/mra.pdf>.

September 2005